Editors' Suggestion

Model for Nonrelativistic Topological Multiferroic Matter

Guidobeth Saez ,[1,2,*] Mario A. Castro,[2,3] Sebastian Allende ,[2,3] and Alvaro S. Nunez [1,2]
[1]*Departamento de Física, Facultad de ciencias físicas y matemáticas, Universidad de Chile, Santiago 8370449, Chile*
[2]*Centro de Nanociencia y Nanotecnología CEDENNA, Avda. Ecuador 3493, Santiago, Chile*
[3]*Departamento de Física, Universidad de Santiago de Chile, 9170124, Santiago, Chile*

(Received 30 May 2023; revised 23 August 2023; accepted 24 October 2023; published 28 November 2023)

We provide a model capable of accounting for the multiferroicity in certain materials. The model's base is on free electrons and spin moments coupled within nonrelativistic quantum mechanics. The synergistic interplay between the magnetic and electric degrees of freedom that turns into the multiferroic phenomena occurs at a profound quantum mechanical level, conjured by Berry's phases and the quantum theory of polarization. Our results highlight the geometrical nature of the multiferroic order parameter that naturally leads to magnetoelectric domain walls, with promising technological potential.

DOI: 10.1103/PhysRevLett.131.226801

Introduction.—Magnetoelectric multiferroics are materials that exhibit magnetic and electric order parameters [1], and their properties have attracted significant attention due to their potential applications in low-dimensional electronic and spintronic devices [2–4]. This potential has fueled a variety of research endeavors, where, for example, a room-temperature magnetoelectric memory was implemented [5].

Multiferroic materials are customarily classified [6] into type-I and type-II multiferroic materials. Type-I multiferroic materials show ferroelectric and magnetic ordering that arise independently [7]. An important example of this type of multiferroics corresponds to $BiFeO_3$. This material offers strong polarization at high temperatures (around 1100 K) and antiferromagnetic ordering at lower temperatures (around 640 K) [8]. Typically, this material achieves a relatively large polarization of 100 $\mu C/cm^2$ [9]. In type II multiferroic materials, the magnetic ordering of the material breaks the inversion symmetry and induces a dipole moment [2]. This is generally achieved through a mechanism that relies on spin-orbit coupling (SOC) as described in [10], although there are alternatives such as the charge order mechanism [11,12] among others [13,14]. For these reasons, such behavior is generally associated with other consequences of the SOC, such as the Dzyalonshinskii-Moriya interaction. In this type of multiferroics, the electrical and magnetic ordering are coupled. Therefore, the magnetic and electric domains and domain walls coexist, and nontrivial magnetoelectric coupling is observed [15]. This type of multiferroics has also been observed in systems of multiferroic heterostructures and 2D van der Waals multiferroic networks [2,16–19].

The quest for generalized magnetoelectric effects is generally guided by the symmetry principles [20]. Examples of this can be found in the literature on the magnetoelectric effect in topological insulators [21] and the discovery of hidden magnetoelectric multipolar order in Cr_2O_3 and α-Fe_2O_3 [22]. Following such guidelines, we present a simplified, nonrelativistic model of a topological multiferroic system. Our chosen model is simple, based on Kronig-Penney's model [23], a well-established framework for studying electronic bands in one dimension. We complement the model by decorating it with magnetic degrees of freedom as localized magnetic moments and considering the coupling between its physical variables [24]. Decoration is set up to explicitly break space inversion $\mathcal{P}$, time reversal $\mathcal{T}$, symmetries, and joint symmetry $\mathcal{PT}$. We investigate the topological phase diagram following the model [25]. We show that the multiferroic behavior of our model arises from the synergy between the magnetic and electric degrees of freedom in the system. Such cooperative interplay takes place deep down at a quantum-mechanical level. It originates from the wavelike behavior of the electron and its Berry phases in what is known as the modern theory of polarization [26]. The strength of the coupling between these two parameters plays a crucial role in determining the properties of the system. We emphasize that no appeal at spin-orbit coupling is drawn at any point in our arguments. Our results provide insight into the behavior of multiferroics, along with hints at the geometrical meaning of the multiferroic order parameter. Our results may help guide the design of new materials with enhanced multiferroic properties. Of particular interest are the two-dimensional van der Waals systems that have been shown to display ferroelectricity [27].

A spin-dependent Kronig-Penney framework.—The essence of the model we studied is as follows. We considered a one-dimensional electronic periodic system described as a nonrelativistic continuum model with period $\mathbf{a}$. Within each unit cell, we have two localized classical spins $\mathbf{S}_1$ and $\mathbf{S}_2$, whose directions we leave as free parameters. Within each unit cell, the local moments are

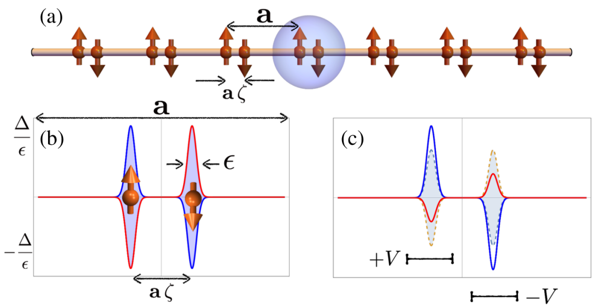

FIG. 1. (a) A cartoon of the model under study. The blue balloon highlights a unit cell of the system. (b) A close-up of a unit cell displays the spin-splitting field's effect on each spin species. The effect of $\delta(\cdot)$ has been smeared by a factor ϵ for illustration purposes. The illustration is made for the case of $V_1 = V_2 = 0$ and $\mathbf{S}_1 = -\mathbf{S}_2$. The red (blue) lines depict the up-spins (down-spins). (c) Same as in (b), but we include a staggered potential $V_1 = -V_2 = V$. The horizontal lines depict these. The image shows that a scalar staggered potential induces a magnetic response.

located at positions $\boldsymbol{\ell}_1$ and $\boldsymbol{\ell}_2$, whose distance is $|\boldsymbol{\ell}_1 - \boldsymbol{\ell}_2| = \mathbf{a}\boldsymbol{\zeta}$, see Fig. 1(a). The dimensionless parameter $0 < \boldsymbol{\zeta} < 1$ will be essential in the following discussions.

The spin-dependent Hamiltonian reads as follows:

$$\mathcal{H} = \frac{p^2}{2m} \mathbb{1}_{\sigma\sigma'} + V_{\sigma\sigma'}(x), \tag{1}$$

where,

$$V_{\sigma\sigma'}(x) = \sum_{n,i} \delta(x - n\mathbf{a} - \boldsymbol{\ell}_i)(V_i \mathbb{1}_{\sigma\sigma'} + \Delta_i \mathbf{S}_i \cdot \boldsymbol{\tau}_{\sigma\sigma'}). \tag{2}$$

Here $\mathbb{1}$ stands for the unit matrix, $\boldsymbol{\tau}$ represents the vector of Pauli's matrices, Δ_i corresponds to an s-d exchange coupling strength, and $\delta(\cdot)$ stands for Dirac's delta signaling the moments' positions, see Fig. 1(b). Regarding electronic filling, although most of our conclusions apply qualitatively to arbitrary occupations, we will consider two cases: one electron per $\delta(\cdot)$ and two electrons per $\delta(\cdot)$. Referring to the effective Hamiltonian discussed later, we call these cases filling one-half and filling one, respectively.

A similar model was used in [28] to reveal topological states in a spinful Su-Schrieffer-Heeger (SSH) nanowire and the spin orbit and Zeeman interactions within such structures. While this model is meant to display symbolic features arising from its symmetries (or lack thereof), we mention in passing that it can provide a faithful account of a family of dimerized one-dimensional antiferromagnets of polymeric nature [29]. Additionally, effective metamaterials [30] can be built in such a way that the glances of this model are cast in their emergent behavior. It is possible to create optical analogs [31,32] whose degrees of freedom follow the dynamics associated with our case study. Finally, we mention the exciting possibility of applying this model to low-dimensional van der Waals magnetic systems such as one-dimensional $\mathrm{MoI_3}$ [33].

We look for solutions in the form of Bloch functions $\Psi_{k\sigma}(x) = u_{k\sigma}(x)e^{ikx}$, where $u_{k\sigma}$ is a periodic function sharing the lattice period and k is a momentum label lying within the first Brillouin zone (BZ).

We numerically diagonalize Eq. (1) and find, in this way, explicit values for eigenvalues $\boldsymbol{\varepsilon}_{mk}$ and eigenvectors $|\mathbf{u}_{mk}\rangle$, where m is a band index and k a momentum label. The Berry phases and spin Berry phases are calculated simultaneously using the following relation:

$$\mathbf{P}_\mu = -\sum_m^{\mathrm{occ}} \oint_{BZ} \frac{\mathrm{d}k}{(2\pi)} \mathrm{Im}\langle \mathbf{u}_{mk}|\sigma_\mu \partial_k|\mathbf{u}_{mk}\rangle, \tag{3}$$

where $\sigma_\mu = (\sigma_0, \boldsymbol{\sigma}_i) = (\mathbb{1}, \boldsymbol{\tau}_i)$. In Eq. (3), occ restricts the sum to the occupied states. We will also consider the spin-polarized Berry's phases: $\mathbf{P}_\uparrow = (\mathbf{P}_0 + \mathbf{P}_z)/2$ and $\mathbf{P}_\downarrow = (\mathbf{P}_0 - \mathbf{P}_z)/2$. $\mathbf{P}_0$ and $\vec{\mathbf{P}}$ are related directly to the electric dipolar density by $\mathcal{P}_e = e\mathbf{a}\mathbf{P}_0$,[26] and the spin-dipolar moment density by $\vec{\mathcal{P}}_s = (\hbar/2)\mathbf{a}\vec{\mathbf{P}}$ [34].

Antiparallel case: A spin-dependent Rice-Mele model.— We address the case $\mathbf{S}_1 = -\mathbf{S}_2$. This choice explicitly breaks the inversion symmetry (around the unit cell midpoint). We choose $\mathbf{S}_1$ as the quantization axis for the electronic spins. We refer to it as the z axis. Diagonal in spin space, we see that model in Eq. (1) reduces to two independent copies of spin complementary replicas. On the first replica, associated with spin-up, one local moment provides a potential well while the other provides a potential barrier. The role of the local moments is reversed in the case of spin-down. We take separately two combinations of V_i.

Case 1: Symmetric potentials: $V_1 = V_2 = 0$. We argue on a permanent spin-dipolar moment and piezospintronic effect.

The system explicitly breaks inversion symmetry, $\mathcal{P}$, and time-reversal symmetry, $\mathcal{T}$. However, the system preserves the combined symmetry $\mathcal{PT}$. We can realize that each spin species in the model is described by an effective Rice-Mele (RM) model [35]. The model exhibits insulating behavior and distinct topological phases. Its spectrum was developed to study the electronic properties of linear polymers [29]. The RM model consists of two-site unit cells with alternating on-site energies $\mathcal{E}_0 + \delta V$ and $\mathcal{E}_0 - \delta V$ and an intra-unit cell hopping matrix element $t + \delta t$. Unit cells are coupled by hopping between cells of the nearest neighbor $t - \delta t$. The case in this section corresponds to $\mathcal{E}_0 \sim 0$, $\delta V \propto \Delta$, and $\delta t(\boldsymbol{\zeta})$. Moreover, the most interesting case of this limit is achieved when one is filled.

The emergence of the spin-dependent RM model as an effective low-energy form from the original model is not an accident, but merely a consequence of the broken and preserved symmetries. For this reason, it allows us to draw several general conclusions. The original spinless RM model is a paradigm of modern polarization theory that attaches a definite value of the electric charge-dipolar moment, $\mathbf{P}_{\uparrow/\downarrow}$, as a function of $\boldsymbol{\zeta}$, and this value, as calculated through the Eq. (3), are odd functions of $\delta V(\propto \Delta)$. The system consists of two replicas with opposite staggered potentials that act on each spin species. This means that $\mathcal{P}_e = e\mathbf{a}(\mathbf{P}_\uparrow + \mathbf{P}_\downarrow)$ vanishes identically and that the system does not have a net charge-dipolar moment. However, the spin-dipolar moment density $\mathcal{P}_z^s = (\hbar/2)\mathbf{a}(\mathbf{P}_\uparrow - \mathbf{P}_\downarrow)$, however, does not cancel. The system exhibits a permanent spin-dipolar moment. This permanent spin-dipolar moment density has doubly degenerate values, presenting two equivalent states connected by time-reversal symmetry.

One might read and control these states by injecting pure spin currents into the system. A desirable goal would be a completely spintronic device, a circuit controlled by spin current that is sensitive to permanent spin-dipolar moments mediated hysteresis loops, reflecting the stability of spin-dipolar moment domains. Spin-carrying domain walls will likely dominate the reversal of such spin-dipolar domains. Such wall dynamics will have a rich phenomenology and be controllable with external fields. Additionally, the above leads to other measurable effects, such as the piezospintronic effect predicted in [34,36], which is the theoretical prediction that certain materials can produce pure spin currents when subjected to mechanical strain. This mechanism to generate pure spin currents could become important in organic spin valves, as shown in [37].

Case 2: Staggered potentials: $V_1 = -V_2 = V$. Here, we present a minimal model of a nonrelativistic multiferroic system. We add a spin-independent scalar staggered potential that alternates between the sites in the system. In this case, the system still explicitly breaks the inversion symmetry $\mathcal{P}$ and the time-reversal symmetry $\mathcal{T}$. However, the system no longer maintains the combined symmetry $\mathcal{PT}$.

Even though the added potential is spin independent, a spin imbalance is induced in the system since the potential favors the electrons in the lower-energy region with a preferred spin direction. See Fig. 1(c). Therefore, the system develops an overall ferromagnetic moment. However, the $\pm V$ correction to the local energy at the sites left unbalanced the Rice-Mele contribution to the electric charge-dipolar moment from each spin species. One is a function of $(\delta V + V)$ and the other of $-(\delta V - V)$. Consequently, there is a nonvanishing net electric charge-dipolar moment density $\mathcal{P}_e = e\mathbf{a}(\mathbf{P}_\uparrow + \mathbf{P}_\downarrow) \neq 0$. See Figs. 2(d) and 2(e).

The model analyzed so far also displays a ferromagnetic moment and a net electric charge-dipolar moment. Hence, it constitutes a simple, nonrelativistic instance of a multiferroic system. These considerations are confirmed by the detailed calculations presented in Fig. 2.

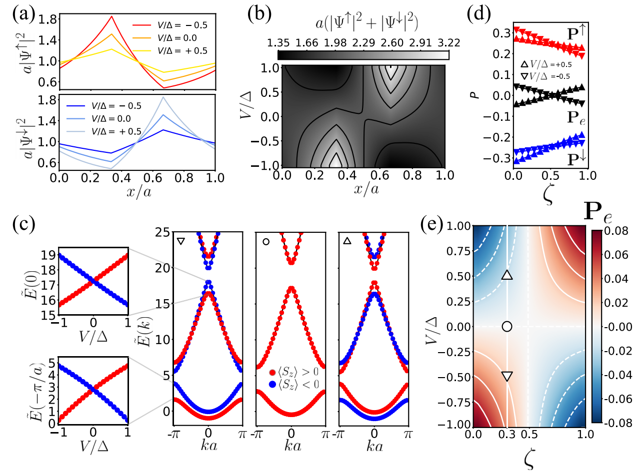

FIG. 2. Antiparallel case with staggered external potential. (a) Wave functions, reflecting the induced spin polarization of the system. (b) Electron density, for the $k = 0$ state, over the unit cell as a function of the staggered potential V. The plot corresponds to $\boldsymbol{\zeta} = 1/3$. (c) Electronic bands $\tilde{E}(k)$, where $\tilde{E}$ stands for E/Δ. In the insets, we see the lowest and highest points of the bands at $k = 0$ and $k = -\pi/a$, as a function of V/Δ. The last two panels are dedicated to the electric polarization of the system. (d) $\mathbf{P}_{\uparrow/\downarrow}$, whose exact cancellation is broken by the presence of V, giving rise to $\mathcal{P}_e$. Up and down triangles represent reversed values of V. (e) $\mathbf{P}_e$ vs V and $\boldsymbol{\zeta}$.

We point out an interesting prediction related to material engineering and design. It is possible to achieve a system with a well-defined gap between the lowest (majority spin) band and the second (minority spin) band. Under the conditions of half-filling, such a system will display quantized magnetization and maximum charge-polarization densities. Large magnetoelectric effects will follow this topologically quantized form of multiferroicity.

As its analogous Hamiltonian (RM), the multiferroic system displays an interesting pattern of charge- and spin-carrying domain walls [38], topological defects that separate lattice regions with different topological properties. For the case studied here, this corresponds to different patterns of dimerization. The multiferroic domain walls will be solitons in that they will show stability and be localized in space [39]. Their propagation can take place without changing their shape significantly, making them potential information carriers. Such solitons will respond easily to external magnetic and electric fields. In the simplified model presented so far, these are independent excitations. However, a glance at the physics of magnon-phonon coupling [40,41] makes the case very compelling that they will indeed be coupled in a real material. The properties of such magnetoelectric solitons should lead to remarkable examples of fractionalization physics, such as that seen in the case of polyacetylene [42,43]. These solitonic domain walls, magnetoelectric in nature, hold promising technological potential.

Discussion and outlook.—In addition to our results with collinear spins, we have tested our ideas with noncollinear arrangements. We report on these results that agree with the basic picture drawn so far in the Supplemental Material [29,38,42,44–55]. We have presented a simplified, nonrelativistic model of a multiferroic system. Our findings indicate that the multiferroic behavior of our model arises from the synergistic interplay between the magnetic and electric degrees of freedom. Such interplay occurs at a deep quantum-mechanical level, determined by Berry's phases and the quantum theory of polarization. Notably, our arguments do not rely on spin-orbit coupling. Our results offer valuable insights into the behavior of multiferroics, including the geometrical significance of the multiferroic order parameter. They will be of aid in the design of new materials with improved multiferroic properties.

The study bears similarities to the spin exchange striction model [56,57] but operates differently. Here, an antiferromagnetic spin order only shows its multiferroic characteristics when exposed to an external potential, producing electric and magnetic properties. There are no mechanical changes, and the parameter $\boldsymbol{\zeta}$ remains constant throughout.

We have referred to a low-energy effective tight-binding Hamiltonian. It can be created by projecting the electronic states into the $\delta(\cdot)$'s bound states and specifying the dynamics by the hopping transitions among them. The specific form can be written after inspection, arriving at an antiferromagnetic generalization of the Rice-Mele Hamiltonian, AFM-RM:

$$\mathcal{H} = -\sum_{i\sigma}\left(\mathrm{t}_i \mathbf{c}^\dagger_{i,\sigma}\mathbf{c}_{i+1,\sigma} + \mathrm{t}^*_i \mathbf{c}^\dagger_{i+1,\sigma}\mathbf{c}_{i,\sigma}\right) + \tilde{\Delta}\sum_{i\sigma\sigma'}(-1)^i \boldsymbol{\tau}^z_{\sigma\sigma'}\mathbf{c}^\dagger_{i,\sigma}\mathbf{c}_{i,\sigma'} + \tilde{V}\sum_{i\sigma}(-1)^i \mathbf{c}^\dagger_{i,\sigma}\mathbf{c}_{i,\sigma}, \quad (4)$$

where $\mathrm{t}_i = \tilde{t} + (-1)^i \widetilde{\delta t}$. In Eq. (4), $\mathbf{c}^\dagger_{i,\sigma}$ ($\mathbf{c}_{i,\sigma}$) stands for a creation (annihilation) operator of an electron at site i with spin component σ. All the parameters with tilde can be easily associated with the original Kronig-Penney model in Eq. (1). A quantitative link can be established by fitting the four lowest bands of that model with those of Eq. (4). This Hamiltonian is easily manageable and easily extended to other dimensions and symmetries. The AFM-Rice-Mele Hamiltonian belongs to the Rice-Mele Hamiltonian family [35,58]. Such a Hamiltonian contains the same low-energy physics as the starting one, Eq. (1), in much fewer degrees of freedom. Interestingly, this Hamiltonian can be regarded as a model for a variety of physical systems ranging from quantum optics, ultracold quantum gases, phononic metamaterials, material sciences, etc.

The model studied in this Letter aims to demonstrate features that result from its symmetries, not to render a direct application to real systems. Nevertheless, it can accurately describe a particular family of polymeric, dimerized, one-dimensional antiferromagnets. Furthermore, by constructing effective metamaterial-based heterostructures, this model can reveal emergent behaviors characteristic of these materials. Furthermore, it is possible to create optical analogs that follow the same dynamics as in our case study. This model can be applied to low-dimensional van der Waals magnetic systems, such as the one-dimensional MoI_3 [33].

Furthermore, our Letter forecasts the possibility of creating a system with a gap between the majority-spin band and the minority-spin band, which would exhibit quantized magnetization and maximal charge-polarization densities. This type of topologically quantized multiferroicity should result in huge magnetoelectric effects.

The model demonstrates the behavior of domain walls that carry charge and spin, known as solitons. These solitons are stable and can be localized in space, moving without significant shape changes, and reacting to external magnetic and electric fields. The coupling of magnons and phonons suggests that these solitons will be connected in real materials, exhibiting properties such as fractionalization physics, as seen in polyacetylene. These magnetoelectric solitons have the potential to be used for information transport and other applications.

The model's generalization to higher dimensions is straightforward and will be a matter of future investigation. In this sense, although our current manuscript focuses on the induction of multiferroics with an electric dipolar moment, we see potential pathways to extend the model to include higher-order multipole moments, such as the quadrupole. By dealing with a 2D version of the SSH [59] and extending it into a 2D AFM-RM model, we can look at the magneto-quadrupolar states. However, we do not expect them to be quantized. A spin extension of the models of [60] could be a path to obtain a quantized magnetoquadrupolar and higher topological order.

On the matter of fluctuations, a common occurrence in many quantum systems, particularly in 1D models, dimerized models, such as our system, are no exception. With quantum- and thermal-symmetry-restoring fluctuations present. When studying the fluctuations around the classical framework tied to the phonon spectrum of the SSH model, it was observed that the zero point motion related to the lattice displacement could be almost on the same scale as the lattice spacing [38]. This realization prompted a reassessment of the traditional classical approximation. Additionally, in particularly small systems, tunneling between equivalent classical configurations can occur swiftly, potentially leading to a consistent ground-state symmetry restoration. Thus, it is crucial to examine whether the broken symmetry of a dimerized system can endure when exposed to quantum tunneling effects. More research is needed on this matter with the specifics of our Hamiltonian.

Quantum tunneling can significantly alter a system, leading to modification of the dimerization order parameter. When evaluating experimental data, this adjusted parameter is vital, especially compared to results from X-ray experiments. Additionally, in optical studies, the optical absorption spectrum will show a peak at the renormalized gap edge. It is crucial to factor in these quantum adjustments when interpreting experimental outcomes.

Quantum fluctuations could potentially alter these topological characteristics, affecting associated physical properties, such as electric polarization. However, as long as the system extension is restricted to protect the dimerization order, the topological polarization will be protected.

Recent experiments involving ultracold quantum gases have made significant progress in achieving integer-quantized topological charge pumping with optical lattices [61], thereby inheriting topological notions in the realm of disordered systems. This has spurred a great deal of research into the effects of static disorder on topological Thouless charge pumping, particularly within the half-filled Rice-Mele model containing random diagonal disorder. It was found that the quantization of transported charge corresponds to the winding of the polarization. Recent ultracold quantum gas experiments have provided evidence to support these findings.

The local moments in this Letter are regarded quenched or frozen. More work is needed if such restrictions were to be lifted. The dynamics of the local moments will enrich the landscape painted so far with spin-transfer torques, magnon-based transport, and spin-pumping effects, in addition to the spin currents that roam the system. Including those degrees of freedom, along with phononic ones, will give rise to various magnetoelectric couplings. These are not apparent in the ideal theory presented here.

Funding is acknowledged from Fondecyt Regular 1230515, 1200867, and Financiamiento Basal para Centros Científicos y Tecnológicos de Excelencia AFB220001. G. S. thanks the financial support provided by ANID Subdirección de Capital Humano/Doctorado, Chile Nacional/2022-21222167. M. A. C. acknowledges Proyecto Postdoc DICYT, Código 042231AP_POSTDOC, Vicerrectoría de Investigación, Desarrollo e Innovación. Powered@NLHPC: This research was partially supported by the supercomputing infrastructure of the National Laboratory for High Performance Computing, Chile (ECM-02).

*guidobethsaez@ug.uchile.cl

[1] N. A. Spaldin and R. Ramesh, Advances in magnetoelectric multiferroics, Nat. Mater. **18**, 203 (2019).

[2] Q. Song, C. A. Occhialini, E. Ergeçen, B. Ilyas, D. Amoroso, P. Barone, J. Kapeghian, K. Watanabe, T. Taniguchi, A. S. Botana, S. Picozzi, N. Gedik, and R. Comin, Evidence for a single-layer van der Waals multiferroic, Nature (London) **602**, 601 (2022).

[3] T. Hu and E. Kan, Progress and prospects in low-dimensional multiferroic materials, WIREs Comput. Mol. Sci. **9**, e1409 (2019).

[4] Y. Gao, M. Gao, and Y. Lu, Two-dimensional multiferroics, Nanoscale **13**, 19324 (2021).

[5] J. T. Heron, J. L. Bosse, Q. He, Y. Gao, M. Trassin, L. Ye, J. D. Clarkson, C. Wang, J. Liu, S. Salahuddin, D. C. Ralph, D. G. Schlom, J. Íñiguez, B. D. Huey, and R. Ramesh, Deterministic switching of ferromagnetism at room temperature using an electric field, Nature (London) **516**, 370 (2014).

[6] *Multiferroic Materials*, edited by J. Wang (CRC Press, Boca Raton, 2016).

[7] G. Giovannetti, D. Puggioni, P. Barone, S. Picozzi, J. M. Rondinelli, and M. Capone, Magnetoelectric coupling in the type-I multiferroic $ScFeO_3$, Phys. Rev. B **94**, 195116 (2016).

[8] R. Ramadan, Study the multiferroic properties of $BiFeO_3/Ni_{0.1}Fe_{2.9}O_4$ for heavy metal removal, Appl. Phys. A **129**, 125 (2023).

[9] P. Rovillain, R. de Sousa, Y. Gallais, A. Sacuto, M. A. Méasson, D. Colson, A. Forget, M. Bibes, A. Barthélémy, and M. Cazayous, Electric-field control of spin waves at room temperature in multiferroic BiFeO3, Nat. Mater. **9**, 975 (2010).

[10] H. Katsura, N. Nagaosa, and A. V. Balatsky, Spin current and magnetoelectric effect in noncollinear magnets, Phys. Rev. Lett. **95**, 057205 (2005).

[11] J. van den Brink and D. I. Khomskii, Multiferroicity due to charge ordering, J. Condens. Matter Phys. **20**, 434217 (2008).

[12] S.-W. Cheong and M. Mostovoy, Multiferroics: A magnetic twist for ferroelectricity, Nat. Mater. **6**, 13 (2007).

[13] M. Fiebig, T. Lottermoser, D. Meier, and M. Trassin, The evolution of multiferroics, Nat. Rev. Mater. **1**, 16046 (2016).

[14] C. Lu, M. Wu, L. Lin, and J.-M. Liu, Single-phase multiferroics: New materials, phenomena, and physics, Natl. Sci. Rev. **6**, 653 (2019).

[15] D. M. Evans, V. Garcia, D. Meier, and M. Bibes, Domains and domain walls in multiferroics, Phys. Sci. Rev. **5**, 20190067 (2020).

[16] C. Huang, J. Zhou, H. Sun, F. Wu, Y. Hou, and E. Kan, Toward room-temperature electrical control of magnetic order in multiferroic van der Waals materials, Nano Lett. **22**, 5191 (2022).

[17] C. Tang and A. Du, Perspective on computational design of two-dimensional materials with robust multiferroic coupling, Appl. Phys. Lett. **122**, 130502 (2023).

[18] J.-J. Zhang, L. Lin, Y. Zhang, M. Wu, B. I. Yakobson, and S. Dong, Type-II multiferroic $Hf_2VC_2F_2$ MXene monolayer with high transition temperature, J. Am. Chem. Soc. **140**, 9768 (2018).

[19] X. Zhang, Z. Zhou, X. Yu, Y. Guo, Y. Chen, and J. Wang, Ferroelectric control of polarity of the spin-polarized current in van der Waals multiferroic heterostructures, Adv. Funct. Mater. **33**, 2301353 (2023).

[20] L. D. Landau, E. M. Lifshitz, and L. P. Pitaevskii, *Electrodynamics of Continuous Media*, 2nd ed., Course of Theoretical Physics (Butterworth-Heinemann, Oxford, England, 1984).

[21] N. P. Armitage and L. Wu, On the matter of topological insulators as magnetoelectrics, SciPost Phys. **6**, 046 (2019).

[22] X. H. Verbeek, A. Urru, and N. A. Spaldin, Hidden orders and (anti-)magnetoelectric effects in Cr_2O_3 and α-Fe_2O_3, Phys. Rev. Research **5**, L042018 (2023).
[23] C. Kittel and P. McEuen, *Introduction to Solid State Physics* (John Wiley & Sons, New York, 2018).
[24] S. J. Blundell, Quasiperiodicity and a spin-dependent kronig-penney model, J. Phys. Condens. Matter **6**, 10283 (1994).
[25] R. Moessner and J. E. Moore, *Topological Phases of Matter* (Cambridge University Press, Cambridge, England, 2021).
[26] D. Vanderbilt, *Berry Phases in Electronic Structure Theory* (Cambridge University Press, Cambridge, England, 2018).
[27] C. Wang, L. You, D. Cobden, and J. Wang, Towards two-dimensional van der Waals ferroelectrics, Nat. Mater. **22**, 542 (2023).
[28] Z.-H. Liu, O. Entin-Wohlman, A. Aharony, J. Q. You, and H. Q. Xu, Topological states and interplay between spin-orbit and zeeman interactions in a spinful Su-Schrieffer-Heeger nanowire, Phys. Rev. B **104**, 085302 (2021).
[29] W. Barford, *Electronic and Optical Properties of Conjugated Polymers* (Oxford University Press, New York, 2013).
[30] G. Go, I.-S. Hong, S.-W. Lee, S. K. Kim, and K.-J. Lee, Realization of Su-Schrieffer-Heeger states based on metamaterials of magnetic solitons, Phys. Rev. B **101**, 134423 (2020).
[31] A. Przysiężna, O. Dutta, and J. Zakrzewski, Rice-Mele model with topological solitons in an optical lattice, New J. Phys. **17**, 013018 (2015).
[32] T. Ozawa, H. M. Price, A. Amo, N. Goldman, M. Hafezi, L. Lu, M. C. Rechtsman, D. Schuster, J. Simon, O. Zilberberg, and I. Carusotto, Topological photonics, Rev. Mod. Phys. **91**, 015006 (2019).
[33] F. Kargar, Z. Barani, N. R. Sesing, T. T. Mai, T. Debnath, H. Zhang, Y. Liu, Y. Zhu, S. Ghosh, A. J. Biacchi, F. H. da Jornada, L. Bartels, T. Adel, A. R. H. Walker, A. V. Davydov, T. T. Salguero, R. K. Lake, and A. A. Balandin, Elemental excitations in MoI_3 one-dimensional van der Waals nanowires, Appl. Phys. Lett. **121**, 221901 (2022).
[34] Á. S. Núñez, Theory of the piezo-spintronic effect, Solid State Commun. **198**, 18 (2014).
[35] M. J. Rice and E. J. Mele, Elementary excitations of a linearly conjugated diatomic polymer, Phys. Rev. Lett. **49**, 1455 (1982).
[36] C. Ulloa, R. E. Troncoso, S. A. Bender, R. A. Duine, and A. S. Nunez, Piezospintronic effect in honeycomb antiferromagnets, Phys. Rev. B **96**, 104419 (2017).
[37] N. Zheng, H. Liu, and Y.-J. Zeng, Dynamical behavior of pure spin current in organic materials, Adv. Sci. Lett. **10**, 2207506 (2023).
[38] A. J. Heeger, S. Kivelson, J. R. Schrieffer, and W. P. Su, Solitons in conducting polymers, Rev. Mod. Phys. **60**, 781 (1988).
[39] C. geun Oh, S.-H. Han, and S. Cheon, Symmetry-protected solitons and bulk-boundary correspondence in generalized Jackiw-Rebbi models, Sci. Rep. **11**, 21652 (2021).
[40] N. Vidal-Silva, E. Aguilera, A. Roldán-Molina, R. A. Duine, and A. S. Nunez, Magnon polarons induced by a magnetic field gradient, Phys. Rev. B **102**, 104411 (2020).
[41] S. Park, N. Nagaosa, and B.-J. Yang, Thermal Hall effect, spin nernst effect, and spin density induced by a thermal gradient in collinear ferrimagnets from magnon-phonon interaction, Nano Lett. **20**, 2741 (2020).
[42] W. P. Su, J. R. Schrieffer, and A. J. Heeger, Solitons in polyacetylene, Phys. Rev. Lett. **42**, 1698 (1979).
[43] R. Jackiw and A. Misra, Fractional charge from topology in polyacetylene and graphene, in *AIP Conference Proceedings* (AIP, Maryland, 2007).
[44] M. Mostovoy, Ferroelectricity in spiral magnets, Phys. Rev. Lett. **96**, 067601 (2006).
[45] A. O. Fumega and J. L. Lado, Microscopic origin of multiferroic order in monolayer NiI_2, 2D Mater. **9**, 025010 (2022).
[46] A. O. Fumega and J. L. Lado, Moiré-driven multiferroic order in twisted $CrCl_3$, $CrBr_3$ and CrI_3 bilayers, 2D Mater. **10**, 025026 (2023).
[47] T. Hirosawa, J. Klinovaja, D. Loss, and S. A. Díaz, Laser-controlled real- and reciprocal-space topology in multiferroic insulators, Phys. Rev. Lett. **128**, 037201 (2022).
[48] S. Park and B.-J. Yang, Topological magnetoelastic excitations in noncollinear antiferromagnets, Phys. Rev. B **99**, 174435 (2019).
[49] S.-W. Cheong and X. Xu, Magnetic chirality, npj Quantum Mater. **7**, 40 (2022).
[50] S.-H. Yang, R. Naaman, Y. Paltiel, and S. S. P. Parkin, Chiral spintronics, Nat. Rev. Phys. **3**, 328 (2021).
[51] Y. Tokura, S. Seki, and N. Nagaosa, Multiferroics of spin origin, Rep. Prog. Phys. **77**, 076501 (2014).
[52] T. Yu, Z. Luo, and G. E. Bauer, Chirality as generalized spin-orbit interaction in spintronics, Phys. Rep. **1009**, 1 (2023).
[53] P. W. Anderson and H. Hasegawa, Considerations on double exchange, Phys. Rev. **100**, 675 (1955).
[54] S. Sachdev, *Quantum Phase Transitions* (Cambridge University Press, Cambridge, England, 2011).
[55] See Supplemental Material at http://link.aps.org/supplemental/10.1103/PhysRevLett.131.226801 for we present an alternative system with multiferroic properties based on non-collinear magnetization. In this case, within one unit cell, the spins of the sites have a non-vanishing vector product $\kappa = s_1 \times s_2$, which is closely related to the chirality of the system [49,50]. We will see that κcan point in any direction, and the system will still generate a non-vanishing polarization. This fact contradicts the basic tenets of the thorough work in [51,52].
[56] I. A. Sergienko, C. Şen, and E. Dagotto, Ferroelectricity in the magnetic e-phase of orthorhombic perovskites, Phys. Rev. Lett. **97**, 227204 (2006).
[57] S. Picozzi, K. Yamauchi, B. Sanyal, I. A. Sergienko, and E. Dagotto, Dual nature of improper ferroelectricity in a magnetoelectric multiferroic, Phys. Rev. Lett. **99**, 227201 (2007).
[58] T. Morimoto, S. Kitamura, and S. Okumura, Electric polarization and nonlinear optical effects in noncentrosymmetric magnets, Phys. Rev. B **104**, 075139 (2021).
[59] F. Liu and K. Wakabayashi, Novel topological phase with a zero berry curvature, Phys. Rev. Lett. **118**, 076803 (2017).
[60] W. A. Benalcazar, B. A. Bernevig, and T. L. Hughes, Quantized electric multipole insulators, Science **357**, 61 (2017).
[61] A. L. C. Hayward, E. Bertok, U. Schneider, and F. Heidrich-Meisner, Effect of disorder on topological charge pumping in the Rice-Mele model, Phys. Rev. A **103**, 043310 (2021).